ORIGINAL ARTICLE

Cell Research (2016) 26:593-612.

www.nature.com/cr

Numb regulates vesicular docking for homotypic fusion of early endosomes via membrane recruitment of Mon1b

Ximing Shao[1, *], Yi Liu[1, 2, 7, *], Qian Yu[1, 2, *], Zhihao Ding[1], Wenyu Qian[2, 3], Lei Zhang[1], Jianchao Zhang[1], Nan Jiang[2, 8], Linfei Gui[1], Zhiheng Xu[5], Yang Hong[6], Yifan Ma[1], Yanjie Wei[1], Xiaoqing Liu[3], Changan Jiang[1, 2], Minyan Zhu[3], Hongchang Li[1], Huashun Li[3, 4]

[1]Shenzhen Key Laboratory for Molecular Biology of Neural Development, Institute of Biomedicine and Biotechnology, Shenzhen Institutes of Advanced Technology, Chinese Academy of Sciences, Shenzhen, Guangdong 518055, China; [2]West China Developmental & Stem Cell Biology Institute, West China Second University Hospital, and State Key Laboratory of Biotherapy, West China Hospital, Sichuan University, Chengdu, Sichuan 610041, China; [3]SARITEX Center for Stem Cell Engineering Translational Medicine, Shanghai East Hospital, Shanghai Tenth People's Hospital, Tongji University School of Medicine, Shanghai 200123, China; [4]ATCG Corp, BioBay, Suzhou Industrial Park, Suzhou, Jiangsu 215123, China; [5]State Key Laboratory of Molecular Developmental Biology, Institute of Genetics and Developmental Biology, Chinese Academy of Sciences, Beijing 100101, China; [6]Department of Cell Biology & Physiology, University of Pittsburgh School of Medicine, Pittsburgh, PA 15261, USA

Numb is an endocytic protein that plays crucial roles in diverse cellular processes such as asymmetric cell division, cell migration and differentiation. However, the molecular mechanism by which Numb regulates endocytic trafficking is poorly understood. Here, we demonstrate that Numb is a docking regulator for homotypic fusion of early endosomes (EEs). Numb depletion causes clustered but unfused EEs, which can be rescued by overexpressing cytosolic Numb 65 and Numb 71 but not plasma membrane-attached Numb 66 or Numb 72. Time-lapse analysis reveals that paired vesicles tend to tether but not fuse with each other in the absence of Numb. We further show that Numb binds to another docking regulator, Mon1b, and is required for the recruitment of cytosolic Mon1b to the EE membrane. Consistent with this, deletion of Mon1b causes similar defects in EE fusion. Our study thus identifies a novel mechanism by which Numb regulates endocytic sorting by mediating EE fusion.

***Keywords*:** Numb; Mon1; early endosome; homotypic fusion

Cell Research (2016) **26**:593-612. doi:10.1038/cr.2016.34; published online 18 March 2016

Introduction

Asymmetric cell division is a fundamental way of generating cell diversity in metazoans, and Numb is the first identified intrinsic determinant of cell fate; mutation of Numb leads to the loss of most of the sensory neurons in the *Drosophila* peripheral nervous system [1-3]. Mammals have two Numb homologs, Numb and Numblike, which play redundant but distinct roles in various cellular processes such as asymmetric cell division, cell differentiation, migration, stem cell activation, adherens junction maintenance, tissue regeneration, tumorigenesis and even Alzheimer's disease-related beta-amyloid precursor protein (APP) cleavage [4-14]. There are at least four major alternatively spliced isoforms of Numb, with different combinations of an 11-amino acid insert in the phosphotyrosine-binding (PTB) domain and a 48-amino acid insert in the proline-rich region, generating four proteins: Numb 65, Numb 66, Numb 71 and Numb 72. Together with Numblike, five proteins are differentially expressed: Numb 65, Numb 66 and Numblike are preferentially expressed in differentiated cells, whereas Numb 71 and Numb 72 are mostly expressed in proliferating cells. Presumably, Numb 65, Numb 66 and Numblike promote

*These three authors contributed equally to this work.
Correspondence: Hongchang Li[a], Huashun Li[b]
[a]E-mail: hc.li@siat.ac.cn
[b]E-mail: huashunli@tongji.edu.cn
[7]Current address: Department of Molecular Genetics, University of Toronto, Toronto, Ontario M5S 1A8, Canada
[8]Current address: Department of Biology, University of Washington, Seattle, Washington, USA
Received 21 July 2015; revised 17 November 2015; accepted 17 January 2016; published online 18 March 2016

cell differentiation, whereas Numb 71 and Numb 72 promote cell proliferation [15, 16]. Different Numb proteins are also distinctly localized to different subcellular compartments: Numb 65, Numb 71 and Numblike are mostly localized in the cytosol, whereas Numb 66 and Numb 72 are mostly localized to the plasma membrane [17], suggesting that different Numb isoforms have distinct roles in different compartments.

Numb localizes to endocytic organelles and participates in both clathrin-dependent and clathrin-independent endocytic trafficking of a number of key molecules such as Notch, EGFR, transferrin, integrin, N-cadherin, E-cadherin and L1 (a neuronal cell adhesion molecule) [9, 17-21]. Genetic evidence shows that Numb contributes to cell fate determination by antagonizing Notch activity in one of the two daughter cells after asymmetric cell division [2, 3, 22]. A recent study suggested that Numb suppresses Notch activity either by facilitating lysosomal degradation of Notch or by reducing its recycling to the plasma membrane [23]. Numb also antagonizes the Notch pathway via facilitating the endocytosis of *Drosophila* sanpodo, which is a membrane protein that is required for Notch activation [24]. These findings suggest that Numb suppresses Notch activity by regulating endosomal trafficking. In addition, Numb controls the intracellular trafficking of APP for membrane recycling and for γ-secretase-mediated cleavage in an isoform-dependent manner; thus Numb may be involved in APP metabolism and Alzheimer's disease pathogenesis [12, 13]. In line with these discoveries, Numb was identified as an endocytic matrix protein [25] and is speculated to function as a homeostatic sensor, which regulates signaling attenuation, termination and maintenance in response to different cellular signals. Although all Numb isoforms bind the clathrin adaptor α-adaptin and other Eps 15-homology domain (EHD)-containing proteins involved in clathrin-dependent and clathrin-independent endocytosis [26-29], the detailed mechanisms by which Numb regulates endocytic trafficking remain to be characterized.

Here, we unexpectedly find that cytosolic Numb is a novel docking regulator for homotypic fusion of early endosomes (EEs). In general, EE homotypic fusion occurs in distinct but consecutive processes, i.e., vesicular tethering, docking, and fusion, and involves multiple proteins including RabGTPases, NSF, a-SNAP, SNAP 25 and EEA1, as well as the SNARE complex [30-35]. Briefly, activated Rab5 drives NSF-primed endosomes to tether and dock with each other via oligomerized EEA1, syntaxin12/13 [32] and possibly the Mon1/CCZ1 complex [36] for subsequent homotypic fusion to generate a fused large endosome. Proteins in the fused large endosomes are either recycled back to the plasma membrane or transported to the trans-Golgi network or lysosome for destruction [37]. We used RNA interference technology [38] to knock down Numb and Numblike to characterize their roles in substrate trafficking. Surprisingly, Numb knockdown (Numb-KD) causes EEs to form a cluster instead of fusing into large vesicles. Time-lapse analysis shows that the endosomes in Numb-KD cells tend to tether to each other but do not fuse. Remarkably, only Numb 65 and Numb 71 can rescue the endosome clustering phenotype in the absence of Numb or promote EE fusion when overexpressed. We further demonstrate that Numb binds to Mon1b, a mammalian homolog of a yeast vacuolar tethering/docking factor Mon1. A mutation in yeast Mon1 impairs cis-SNARE complex assembly and the subsequent trans-SNARE pairing [36]. Loss of Numb blocks cytosolic Mon1b from being recruited to EEA1-positive vesicles. Thus, our study has identified cytosolic Numb as a novel docking regulator required for recruiting cytosolic Mon1b to EEA1-positive vesicles for homotypic fusion, suggesting that Numb may regulate multiple critical events such as endocytosis, recycling and degradation of proteins to fine-tune signaling strength and duration in a variety of physiological processes.

Results

Mammalian Numb is required for homotypic fusion of early endosomes

To characterize the detailed mechanisms underlying Numb-mediated endocytic trafficking, we used two short hairpin RNAs (shRNAs) to knock down Numb expression in MCF7A cells (Figure 1A) and performed anti-EEA1 immunofluorescence staining to examine the EEs. Compared with control cells, most EEA1-positive EEs concentrated and formed large clusters (≥ 2 vesicles) in the perinuclear region of Numb-KD cells. Interestingly, EE clusters in Numb-KD cells were organized in linear arrays (Figure 1B). As EEs are known to be associated with F-actin [39-41], the linear arrangement of clustered EEs suggests that the EE clusters most likely bind to F-actin. Quantification showed that > 70% of EEs formed clusters in Numb-KD cells, whereas only half of EEs appeared as clusters in control cells (Figure 1C). Notably, more than 30% of EE clusters consisted of ≥ 5 endosomes and only ~27% of EE clusters contained 2 endosomes in Numb-KD cells, whereas ~50% of EE clusters had only 2 endosomes in control cells (Figure 1D). By using transmission electron microscopy (TEM), we further found that Numb KD did not affect EE morphology but greatly increased the vesicle numbers (Figure 1E). Vesicle size distribution analysis revealed that

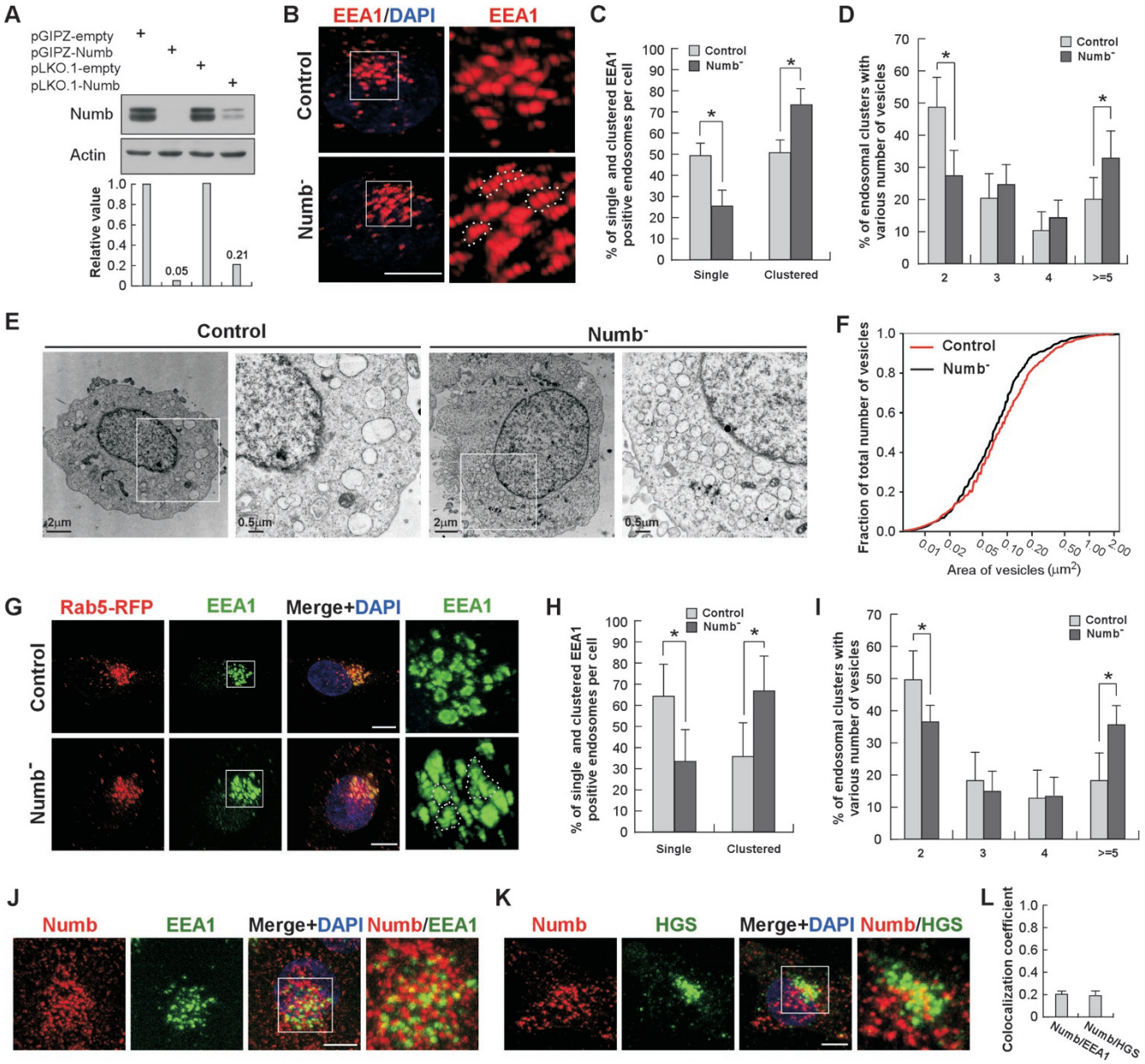

Figure 1 Numb knockdown induces EE clustering. **(A)** Western blot showing transfection of shRNA (pGIPZ-Numb or pLKO1-Numb) targeting Numb efficiently knocks down Numb expression. Bottom panel shows Numb expression normalized by β-actin protein level. **(B-D)** Control and Numb-KD MCF7A cells are stained with anti-EEA1 antibodies. Representative images are shown in **B** and areas within the white squares are enlarged on the right. Clustered EEA1-positive EEs in Numb-KD cells are outlined by dotted line and quantified in **C** and **D** (n = 30 cells). **(E)** Electron micrographs of control and Numb-KD MCF7A cells. Areas within the white squares are enlarged on the right. Endocytic vesicles are identified based on their unique membrane projections and lack of internal electron density. **(F)** Size distribution of vesicles based on electron micrographs of control and Numb-KD cells (n = 10 cells, P = 0.0316). **(G-I)** Control and Numb-KD MCF7A cells expressing Rab5-RFP are stained with anti-EEA1 antibody. Representative images are shown in **G**. Quantification of the clustered EEs is shown in **H** and **I** (n = 30 cells). **(J-L)** MCF7A cells are co-stained with antibodies against Numb and EEA1 **(J)** or Numb and HGS **(K)**. Co-localization coefficients of Numb and EEA1, and Numb and HGS are shown in **L** (n = 5 cells). The Numb-depleted MCF7A cells in **B-I** are obtained by transfection of pGIPZ-Numb, and cells expressing pGIPZ-empty serve as control. Scale bars in **B**, **G**, **J** and **K**, 5 μm. *P < 0.01.

Numb-KD cells contained fewer large vesicles and more small vesicles compared with control cells (Figure 1F), very likely owing to reduced vesicle fusion. Of note, Numb depletion-induced EE clustering was confirmed in several other cell lines and primary cells (Supplementary information, Figure S1). These data suggest that Numb may play a general role in EE homotypic fusion. We further validated the Numb KD-induced defects in EE fusion by using another shRNA that also dramatically reduces Numb expression (Figure 1A and Supplementary information, Figure S2). This strongly suggests that the defects in EE fusion are specifically due to the lack of Numb expression.

Mammals contain two Numb homologs, Numb and Numblike, which play both redundant and distinct roles in various cellular processes [4, 5, 9]. Thus, we also examined the effect of Numblike KD on EE fusion. Numblike-KD cells did not show obvious defects in EE fusion, suggesting that Numblike has little or no function in the homotypic fusion of EEs (Supplementary information, Figure S3).

Rab5 is a well-documented docking/fusion factor for EE maturation. Next, we asked whether Numb-mediated EE fusion is Rab5-dependent or Rab5-independent. Consistent with previous reports [30, 42], Rab5 overexpression produced a large number of giant EEs. However, Numb KD completely blocked Rab5-mediated formation of giant EEs (Figure 1G-1I), suggesting that Numb may act downstream of Rab5 signaling. By using a previously developed Rab5 activity assay [43], we further determined that Numb KD had no striking effect on Rab5 activity (Supplementary information, Figure S4A-S4C). Thus, our data uncover a novel function of Numb in EE homotypic fusion. In line with these findings, Numb is partially co-localized with EE proteins EEA1 and HGS on EEs (co-localization coefficient of ~0.2; Figure 1J-1L).

Numb is a docking regulator for EE fusion

Homotypic fusion of EEs proceeds in three consecutive and discernible steps: tethering, docking and fusion [31]. To precisely determine at which step Numb controls homotypic fusions, we performed live imaging analysis to investigate this dynamic fusion process. To visualize the endocytic vesicles, cells were first incubated with DiI-LDL or Alexa-555-conjugated transferrin, which is internalized by the cells, and then quickly subjected to time-lapse imaging [44]. As expected, three distinct steps during the endosome fusion process, tethering, docking and fusion, were observed in control cells (Figure 2A and Supplementary information, Movie S2). In contrast, EEs in Numb-KD cells were capable of moving to the perinuclear region but were unable to proceed to fusion. Remarkably, these clustered EEs were not stably docked but rapidly oscillated around each other (Figure 2A and Supplementary information, Movie S2), suggesting that the defect occurred before the fusion step but after the tethering step because otherwise the clusters would move away if not tethered. Next, we further analyzed the EE behavior. The vesicles recorded were classified into three groups: randomly running endosomes, which neither oscillated around nor fused with each other; tethering endosomes, which performed long-term oscillations (at least five cycles of kiss and run) around each other in a very narrow range (500-1 000 nm); and docking/fused endosomes, which physically associated or further fused with each other at the end of chased period (Supplementary information, Figure S5A and Movie S1). We found that Numb depletion did not affect the randomly running endosomes. However, Numb depletion dramatically increased the number of tethering endosomes and decreased the number of docking/fusion endosomes, indicating that Numb depletion severely impaired the process from tethering to fusion, very likely the docking step (Figure 2B). The similar phenotype caused by Numb KD was confirmed by tracing transferrin-labeled EEs (Figure 2C, Supplementary information, Figure S5B and Movie S3). Because transferrin is recycled via recycling endosomes and LDL is degraded via lysosomes, involvement of Numb in both endocytic processes therefore suggests that Numb plays a general role in EE docking process. It should be noted that Numblike knockdown showed no obvious effect on EE dynamics (Figure 2A-2C, Supplementary information, Figure S5B, Movies S2 and S3), further indicating that only Numb, but not Numblike, plays roles during EE fusion.

To validate that Numb regulates EE docking in a ubiquitous manner, we further examined the effect of Numb KD on Rab5-positive EEs in Rab5-RFP-expressing cells. We found that ~70% of Rab5-positive vesicles were capable of completing the entire fusion process, tethering, docking and fusion, in control cells (Figure 2D, 2E and Supplementary information, Movie S4). Strikingly, Numb KD reduced the percentages of EEs that completed the fusion process to ~36%, and most of the observed EEs were rapidly oscillating with each other in a very narrow range, presumably at the tethering distance, in the chasing period (Figure 2D, 2E and Supplementary information, Movie S4), indicating that the docking process between these EEs was impaired. These data support that Numb is a critical docking regulator for EE fusion.

Cytosolic Numb 65 and Numb 71 regulate homotypic fusion of EEs

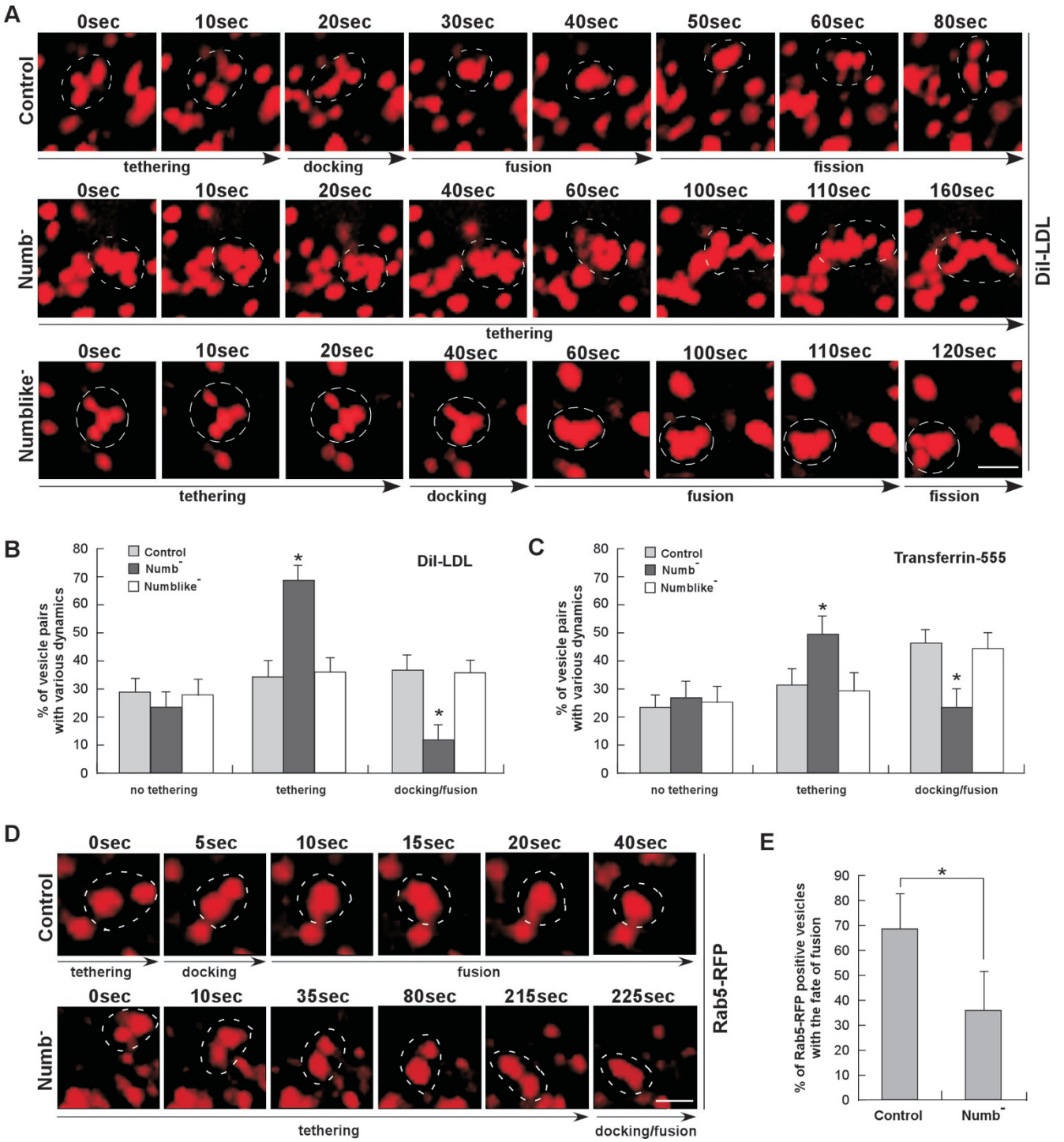

Figure 2 Numb knockdown causes EE docking defects. **(A**, **B)** Fusion of endocytic vesicles in Dil-LDL-labeled control, Numb KD and Numblike KD MCF7A cells visualized by time-lapse video microscopy. Dashed lines outline representative vesicles undergoing fusion **(A)**. Percentages of Dil-LDL-positive vesicles at different phases of fusion (random movement, tethering and docking/fusion) in control and Numb-depleted cells (**B**, *n* = 15 cells). **(C)** Percentages of transferrin-555-positive vesicles at different phases of fusion in control and Numb-depleted cells based on time-lapse video microscopy (*n* = 15 cells). **(D**, **E)** Time-lapse video microscopy of control and Numb-depleted MCF7A cells transfect with Rab5-RFP which labels vesicles undergoing fusion **(D)**. Percentages of vesicles that complete fusion (**E**, *n* = 20 cells). Numb-depleted MCF7A cells are obtained by transfection of pGIPZ-Numb, and cells expressing pGIPZ-empty serve as control. Scale bar, 500 nm. **P* < 0.01.

In contrast to *Drosophila* which has only one form of Numb, mammals have four alternatively spliced isoforms of Numb (Numb 65, Numb 66, Numb 71 and Numb 72) and Numblike, each localized in a distinct set of subcellular compartments and presumably performing compartment-specific functions [15]. We wondered whether all these molecules are involved in EE homotypic fusion. Here, we show that overexpression of cytosolic Numb 65 and Numb 71, both lacking an insertion in the PTB domain, produced giant EEA1-positive endosomes, presumably due to increased fusion of EEs, whereas overexpression of Numb 66 and Numb 72 did not have obvious effects on EE fusion, and overexpression of Numblike had only a moderate effect (Figure 3A-3D). Furthermore, we found that only expression of Numb 65 and Numb 71 could rescue the Numb depletion-induced EE docking defects (Figure 3E-3H). These data indicate that only cytosolic Numb 65 and 71 regulate EE docking/fusion.

Consistent with the above findings, only Numb 65 and Numb 71 were found to be enriched in perinuclear EEs (Figure 3A). A previous report showed that the presence of the insertion in the PTB domain influences of Numb's localization [15]. Thus, we examined whether the short PTB domain is responsible for EE recruitment of Numb. To this end, we generated various myc-tagged Numb truncation constructs (Supplementary information, Figure S6A). We found that the PTB domain without the insertion was predominantly localized in the cytosol and nucleus and partially co-localized with EEs. In contrast, the PTB domain with the insertion is mostly localized on the plasma membrane but not on EEs (Supplementary information, Figure S6B and S6C). Conversely, the Numb 71 mutant lacking the PTB domain completely lost recruitment to EEs but significantly accumulated on AP2-positive endocytic vesicles (Supplementary information, Figure S6D and S6E). Taken together, these data strongly indicate that the PTB domain of Numb is essential for Numb's localization on EEs. In line with these findings, we further identified that amino acids 69-171 of Numb 71 may constitute the core domain for Numb recruitment to EEs as a truncated PTB domain lacking the N-termial 68 aminal acids showed much stronger EE localization than the WT PTB fragment (Supplementary information, Figure S6F and S6G).

To clearly understand the relationship between Numb and Rab5 during EE fusion, we overexpressed Numb along with different forms of Rab5 in MCF7A cells. Expression of either wild-type Rab5 or a constitutively activated mutant (Q79L) of Rab5 had almost no effect on Numb-induced EE fusion, but expression of a dominant-negative mutant (S34N) of Rab5 completely abolished the Numb-induced EE fusion, suggesting that Numb-induced EE fusion requires Rab5 activity (Supplementary information, Figure S4D-S4F). Notably, expression of Rab5 Q79L significantly facilitated the recruitment of Numb 65 and Numb 71 to the giant EEs, further indicating that EE recruitment of Numb probably requires Rab5 activity (Supplementary information, Figure S4E).

To definitively prove the role of Numb in EE docking/fusion, we applied a previously developed *in vitro* vesicle fusion assay [45]. Briefly, endocytic vesicles were labeled by internalization of transferrin-488 or transferrin-555 at 37 °C for 5 min. The postnuclear supernatant (PNS) preparation containing labeled vesicles and cytosolic preparation containing soluble factors were isolated and used for the subsequent *in vitro* fusion reactions (Figure 4A). The amount of fusion is determined by examining double-labeled vesicles after the reaction is terminated.

We tested two concentrations of PNS (1 and 2 μg/μl) in our *in vitro* assays. Using cytosolic and PNS fractions from Numb KD cells dramatically reduced the number of fused vesicles by ~50% compared with control reactions after a 40-min incubation at 37 °C (Figure 4B and 4D), even if equal numbers of vesicles were employed in the assays before the temperature is shifted to 37 °C (Figure 4B and 4C). We followed the vesicle fusion during the 40-min period and found that the number of fused vesicles increased gradually in control reaction, whereas the vesicle fusion was greatly reduced in Numb KD reaction (Figure 4E). We also found that the number of vesicles larger than 2.0 μm^2 was remarkably reduced in the Numb KD reaction (Figure 4F), most likely result of slow vesicle fusion. These data further support the idea that Numb has a crucial function in vesicle fusion. In these assays, Numb KD also significantly reduced the number of vesicles smaller than 0.5 μm^2, suggesting that Numb KD may also impair the vesicle fission process (Figure 4F). Importantly, the reaction using control cytosolic fraction and Numb KD PNS or Numb KD cytosolic fraction and control PNS generated vesicle fusion rates (Figure 4B and 4E) and vesicle sizes (Figure 4F) similar to the control reaction, suggesting that Numb from either the cytosolic or the PNS fraction can support EE fusion.

Numb interacts with mammalian Mon1a and Mon1b in vivo

We next carried out co-immunoprecipitation assays to search for potential cytosolic factors through which Numb regulates EE docking. We selected twelve proteins that have been previously characterized for their function in vacuole fusion. Among them, Mon1b, a mammalian homolog of a yeast vacuolar tethering/docking factor

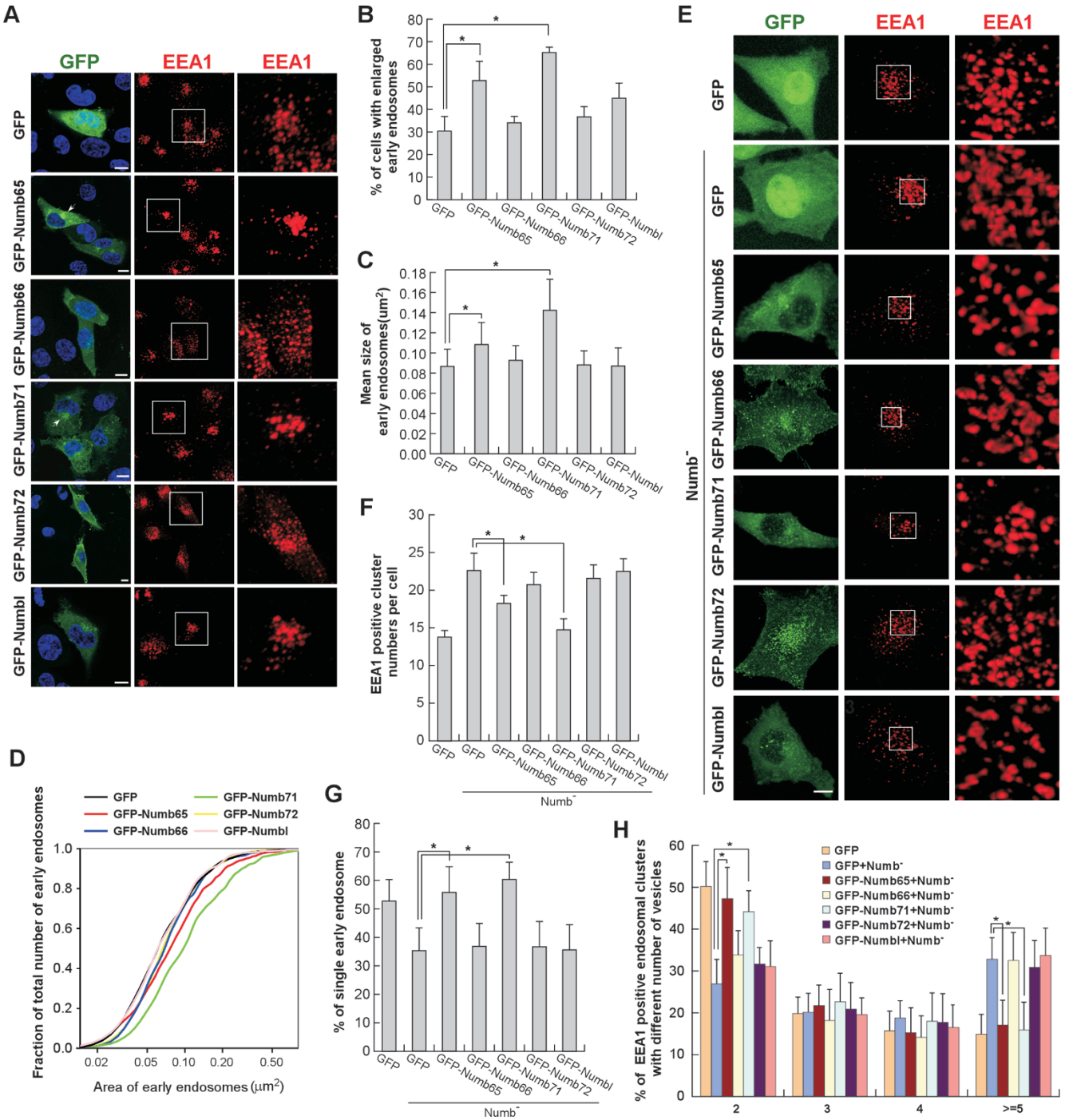

Figure 3 Numb 65 and Numb 71 are required for EE fusion. **(A-D)** MCF7A cells transfected with GFP or various GFP-tagged Numb isoforms are stained with anti-EEA1 antibody. Representative images are shown in **A**. Areas in white squares are enlarged on the right. Arrowheads indicate perinuclear localization of GFP-Numb 65 and GFP-Numb 71. Percentages of cells with enlarged EEs (**B**, $n \geq 20$ cells), mean size of EEs (**C**, $n \geq 20$ cells) and size distribution of EEs (**D**, $n \geq 20$ cells, $P = 1.58E{-}05$ for Numb 65, $P = 4.46E{-}20$ for Numb 71) upon expression of different Numb isoforms. **(E-H)** Anti-EEA1 immunostaining of MCF7A cells stably expressing pLKO.1-Numb and transiently expressing GFP or various GFP-Numb isoforms. Representative images are shown in **E**. Average number of EEA1-positive EE clusters per cells (**F**, $n \geq 20$ cells), percentages of single EEs (**G**, $n \geq 20$ cells), and size distribution of EEA1-positive endosomal clusters (**H**, $n \geq 20$ cells). Scale bar, 5 μm. *$P < 0.01$.

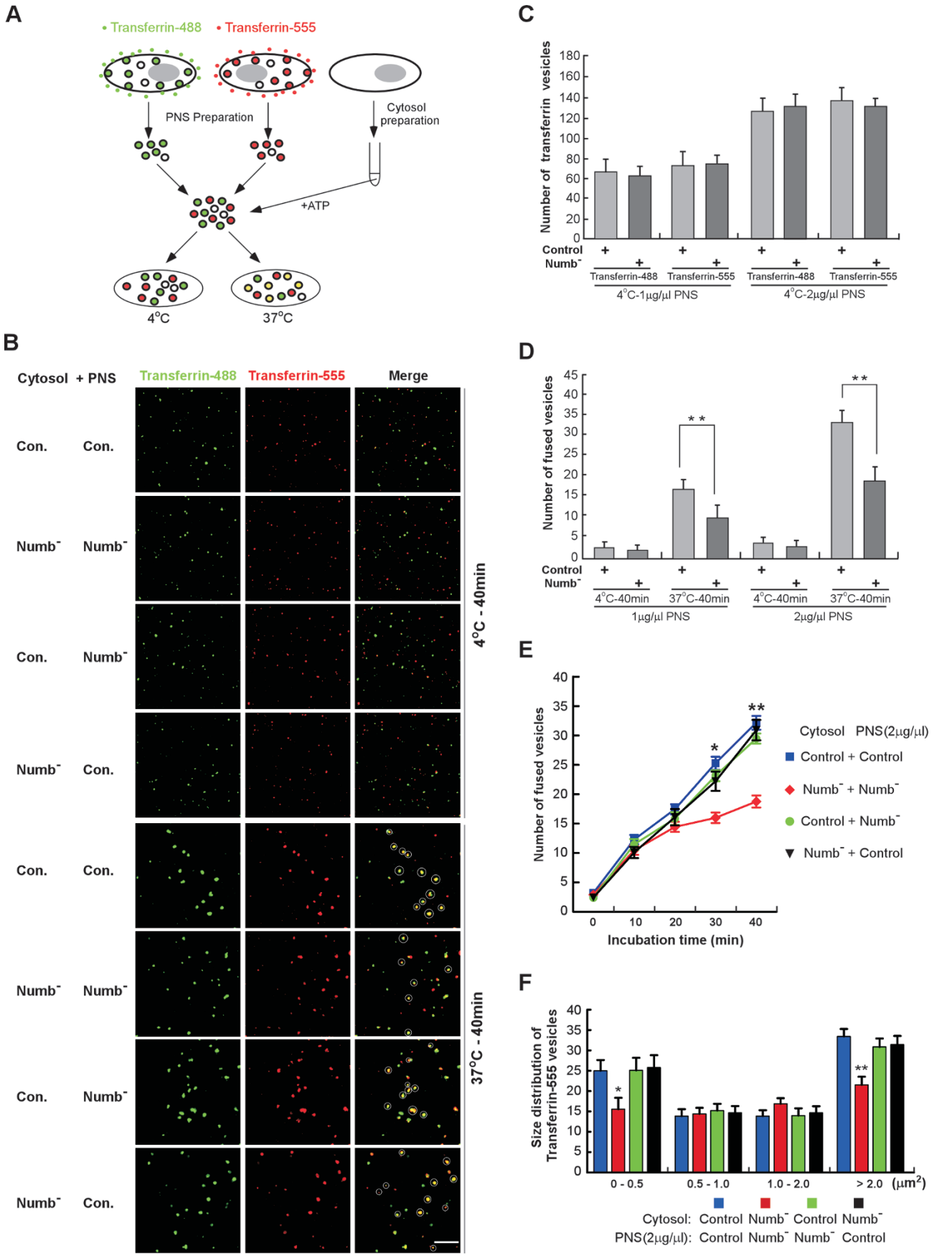
A
• Transferrin-488 • Transferrin-555
PNS Preparation
Cytosol preparation
+ATP
4°C
37°C
B
Cytosol + PNS
Transferrin-488
Transferrin-555
Merge
Con. Con.
Numb⁻ Numb⁻
Con. Numb⁻
Numb⁻ Con.
Con. Con.
Numb⁻ Numb⁻
Con. Numb⁻
Numb⁻ Con.
4°C - 40min
37°C - 40min
C
Number of transferrin vesicles
Control
Numb⁻
Transferrin-488
Transferrin-555
Transferrin-488
Transferrin-555
4°C-1μg/μl PNS
4°C-2μg/μl PNS
D
Number of fused vesicles
Control
Numb⁻
4°C-40min
37°C-40min
4°C-40min
37°C-40min
1μg/μl PNS
2μg/μl PNS
E
Number of fused vesicles
Incubation time (min)
Cytosol PNS(2μg/μl)
Control + Control
Numb⁻ + Numb⁻
Control + Numb⁻
Numb⁻ + Control
F
Size distribution of Transferrin-555 vesicles
0 - 0.5
0.5 - 1.0
1.0 - 2.0
> 2.0 (μm²)
Cytosol: Control Numb⁻ Control Numb⁻
PNS(2μg/μl): Control Numb⁻ Numb⁻ Control

Figure 4 Numb regulates EE docking/fusion *in vitro*. **(A)** Schematic overview of the *in vitro* vesicle fusion assay. MCF7A cells are divided into two aliquots; one is incubated with Transferrin-488 for 5 min at 37 °C, and the other with Transferrin-555 under the same condition. Postnuclear supernatants (PNSs) of both aliquots are mixed and incubated in the presence of ATP, buffer, and cytosol (either from control cells or Numb KD cells) at 4 °C or 37 °C for various times. The reaction product is centrifuged onto a coverslip and imaged. The amount of fusion is determined by measuring the production of double-labeled vesicles after reaction. **(B)** Representative fluorescence images from various reactions at 4 °C or 37 °C. Fused vesicles are marked with yellow circles. **(C**, **D)** Numbers of different transferrin-labeled vesicles at 4 °C **(C)** or after a 40-min reaction either at 4 °C or 37 °C **(D)**. Control: control PNS + control cytosol; $Numb^{-}$: $Numb^{-}$ PNS + $Numb^{-}$ cytosol. The data are extracted from at least 40 microscopic fields from three independent experiments. **(E)** Time course of vesicle fusion in different conditions. The data are extracted from at least 40 microscopic fields from three independent experiments. **(F)** Size distributions of Transferrin-555-containing vesicles after a 40-min vesicle fusion reaction at 37 °C. The data are extracted from at least 40 microscopic fields from three independent experiments. Scale bar, 100 μm. **P* < 0.05; ***P* < 0.01.

Mon1, specifically bound to Numb71 (Supplementary information, Figure S7A). We further found that both Mon1a and Mon1b, two mammalian homologs of yeast Mon1, were associated with endogenous Numb (Figure 5A and 5B). Further analysis showed that amino acids 240-311 of Numb were required for interaction between Numb and Mon1 proteins (Supplementary information, Figure S7B-S7E). Surprisingly, all Numb isoforms and Numblike bound to Mon1a and Mon1b (Supplementary information, Figure S7F and S7G), although only Numb 65 and Numb 71 function in EE docking, suggesting that Numb and Mon1 interactions may have broader roles in a variety of cellular processes.

Numb recruits Mon1b from the cytoplasm to EEs

We next asked whether Numb regulates vesicular fusion via Mon1. Immunofluorescence staining shows that Numb KD dramatically reduced the punctate signals of both Mon1a (~57% reduction) and Mon1b (~37% reduction; Supplementary information, Figure S8A-S8D). The altered subcellular distribution pattern of Mon1a after Numb KD was confirmed by overexpression of Mon1a-myc and Mon1a-GFP proteins (Supplementary information, Figure S8E-S8G). Interestingly, only Mon1b, but not Mon1a, was detected on Rab5-RFP or EEA1-labeled EEs (Figure 5C-5F and Supplementary information, Figure S8H), suggesting that only Mon1b is relevant to EE docking. Thus, we tested whether Numb contributes to Mon1b localization on EEs. As shown in Figure 5F and 5G, Numb KD significantly reduced the localization of Mon1b on EEs in MCF7A cells. To validate this effect of Numb KD on Mon1 recruitment to the EE membrane, we further purified EEs. In line with our immunofluorescence staining data, Mon1b, but not Mon1a, was detected in isolated EEs, and Numb KD significantly reduced the amount of Mon1b on these EEs (Figure 5H). Of note, Numb KD did not affect the overall protein expression of Mon1a and Mon1b (Figure 5H). Taken together, these data suggest that Numb is required for Mon1b recruitment to EEs, which may be a major mechanism by which Numb regulates EE docking. Although Mon1a was not detected on EEs, we noticed that Numb KD also reduced the punctate signals of Mon1a (Supplementary information, Figure S8A, S8B, S8E-S8G), suggesting that Numb may regulate Mon1a in other cellular processes than EE fusion.

Mon1b is an essential docking factor for EE fusion

The yeast Mon1 is crucial for vacuolar tethering/docking [36], but the role of its mammalian homolog in EE fusion is unknown. By using RNA interference [38], we knocked down Mon1a and Mon1b (Figure 6A and Supplementary information, Figure S9A and S9B). Mon1a KD had no effect on EE fusion (Figure 6B-6D and Supplementary information, Figure S9C-S9E), whereas depletion of Mon1b blocked EE fusion, as evidenced by the drastic accumulation of EEA1-positive vesicle clusters (~75% increase; Figure 6E-6G). We then performed time-lapse analysis. Similar to the EEs in Numb KD cells, EEs in Mon1b KD cells remained tethered for extended periods of time instead of proceeding to docking and fusion, whereas EEs in Mon1a KD cells fused like those control cells (Figure 6H, 6I and Supplementary information, Movie S5). All these data suggest that only mammalian Mon1b, but not Mon1a, has a conserved function in vesicular docking. Consistently, transmission electron microscopy assays showed that more smaller endocytic vesicles in Mon1b KD cells than in control cells (Figure 6J and 6K), similar to what was observed in Numb KD cells, indicating that both Numb and Mon1b are critical regulators of vesicle fusion.

We also investigated the effect of Numb/Mon1b KD on late endosomes and recycling endosomes. Numb KD had no effect on Rab7-labeled late endosome and Lamp1-labeled lysosome, whereas Mon1b KD caused significant aggregation of late endosomes in the perinuclear region (Supplementary information, Figure S10A-S10B). These data are consistent with the previously de-

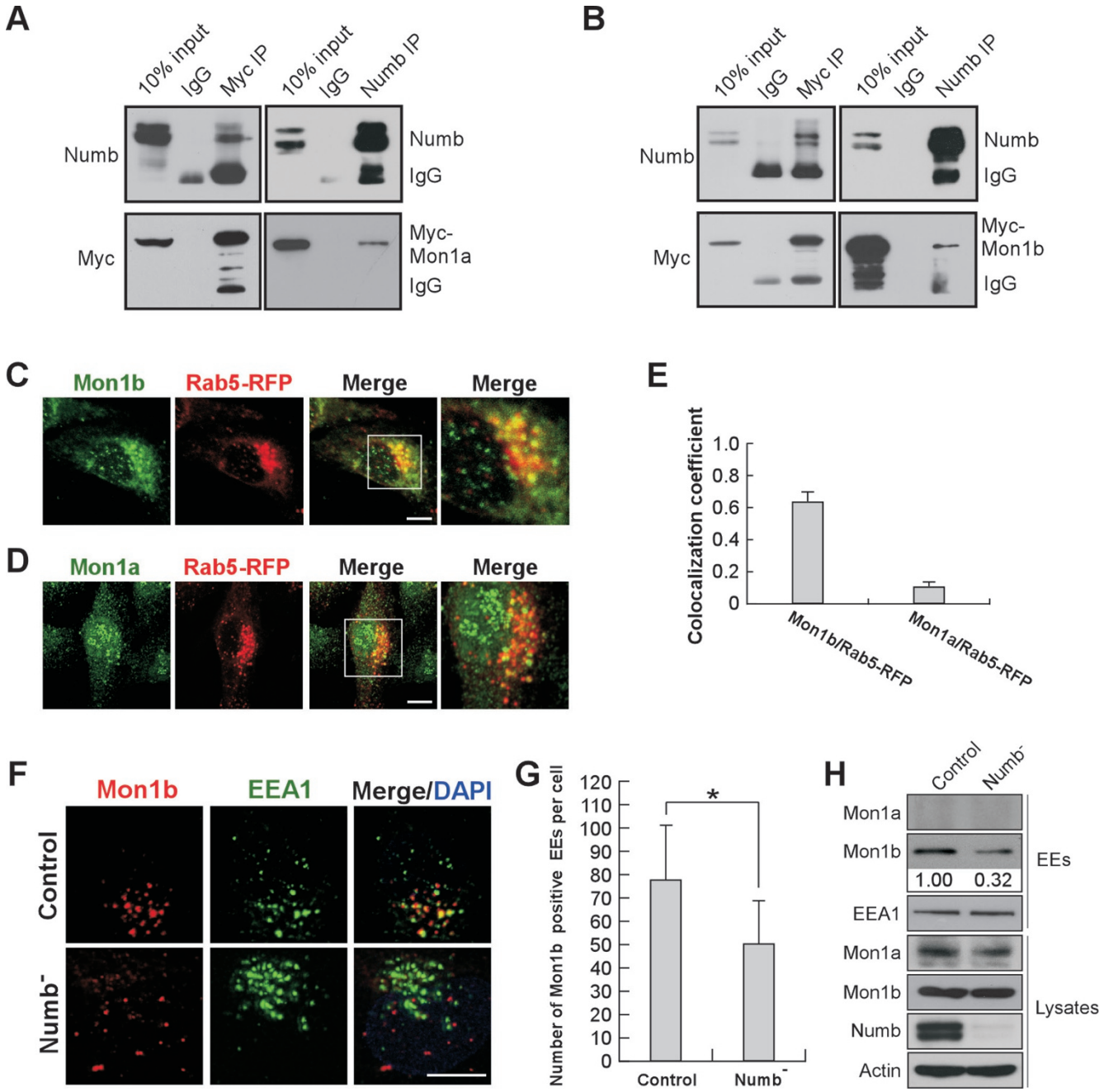

Figure 5 Numb is required for the recruitment of Mon1b to EEs. **(A**, **B)** Co-immunoprecipitation assay of MCF7A cells transfected with Myc-Mon1a **(A)** or Myc-Mon1b **(B)**. **(C**-**E)** Immunostaining of MCF7A cells transfected with Rab5-RFP with antibody against Mon1b **(C)** or Mon1a **(D)**. Co-localization coefficients of Mon1b, and Mon1a with Rab5-RFP (**E**, *n* = 5 cells). **(F**, **G)** Immunostaining of control and Numb KD MCF7A cells with anti-Mon1b and anti-EEA1 antibodies **(F)**. Numb KD reduces the number of Mon1b-positive puncta (**G**, *n* = 60 cells). **(H)** EEs in control and Numb KD MCF7A cells are immunoisolated using anti-EEA1 antibody and subjected to immunoblotting. Densitometric values for Mon1b in EEs are shown below the bands. The Numb-depleted MCF7A cells in these experiments are obtained by transfection of pLKO.1-Numb, and cells expressing pLKO.1-empty serve as control. Scale bar, 5 μm. *P < 0.01.

scribed function of Mon1b in late endosome maturation [46, 47]. As Numb KD does not affect late endosomes, the function of Mon1b in late endosome maturation is very likely Numb-independent. We further found that

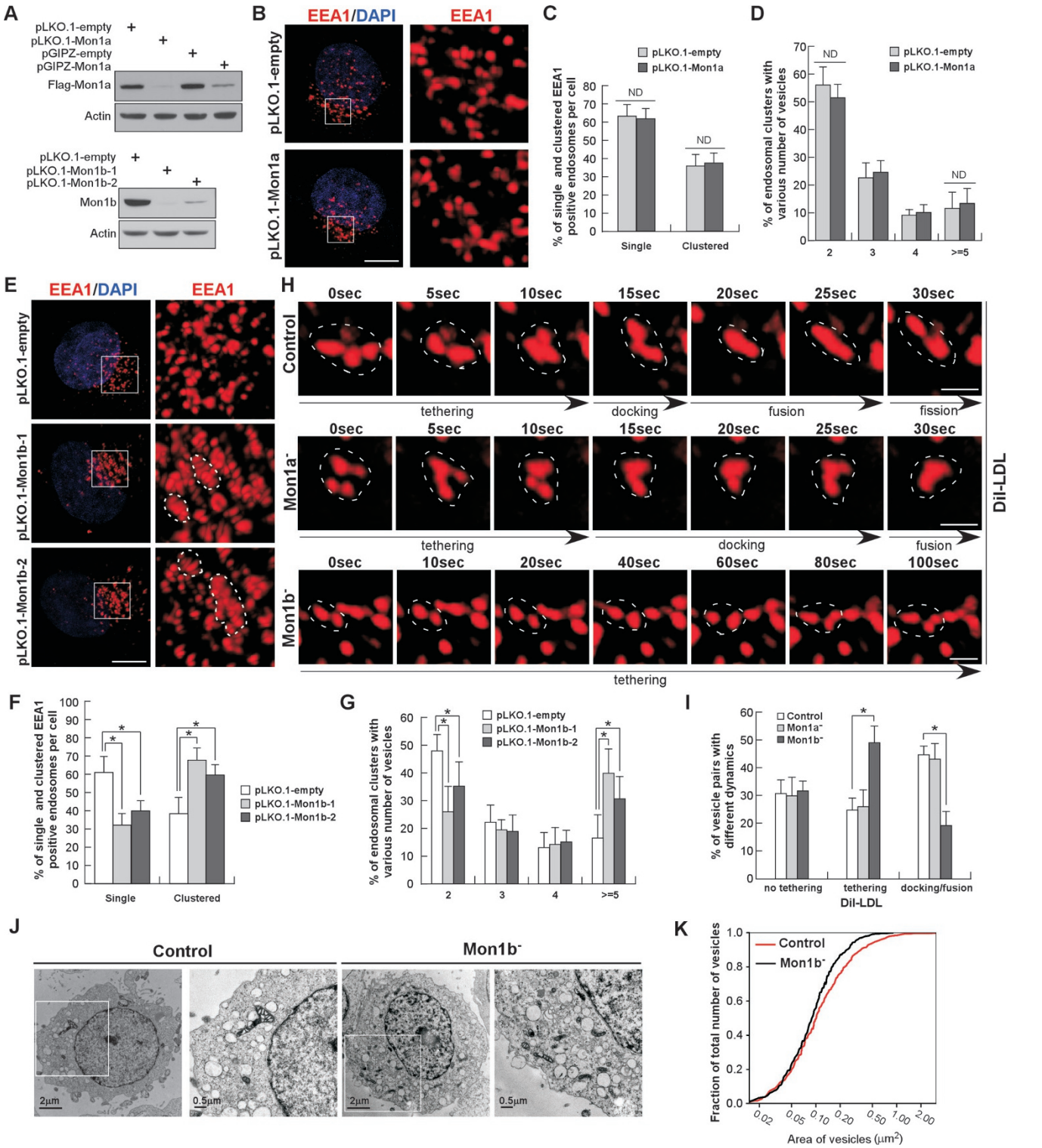

Figure 6 Knockdown of Mon1b, but not Mon1a, perturbs vesicular docking during EE fusion. **(A)** Depletion of Mon1a and Mon1b via shRNA. **(B-G)** Control and Mon1a- **(B)** or Mon1b- **(E)** depleted MCF7A cells are stained with anti-EEA1 antibody. Dashed lines mark the EE clusters. Quantifications are performed as in Figure 1 and the results are shown in **C**, **D**, **F** and **G** (n = 30 cells). **(H**, **I)** Time-lapse video microscopy of control and Mon1a- or Mon1b-depleted MCF7A cells labeled with Dil-LDL (n = 30 cells). **(J**, **K)** Electron micrographs of control and Mon1b-KD MCF7A cells **(J)**. Endocytic vesicles are identified and quantified as in Figure 1 and the results are shown in **K** (n = 10 cells, P = 1.0966E-06). Scale bars in **B** and **E**, 5 μm; scale bars in **H**, 500 nm. *P < 0.01. ND, no significant difference.

Numb/Mon1b KD had no effect on the Rab4-positive fast recycling endosomes (Supplementary information, Figure S10C), and Numb KD, but not Mon1b KD, caused striking perinuclear accumulation of Rab11-positive slow recycling endosomes (Supplementary information, Figure S10D), suggesting that Numb has a Mon1b-independent function in slow recycling endosome maturation or trafficking. Taken together, these observations suggest that Numb and Mon1b may have additional independent roles other than regulating EE fusion in endocytic trafficking.

Numb-mediated regulation of EE docking depends on Mon1b

To determine the relationship of Numb and Mon1 in EE docking, we examined the EE fusion events in Mon1b KD MCF7A cells overexpressing various Numb isoforms and Numblike. Overexpression of all Numb isoforms in Mon1b KD cells did not induce fusion of EEs above control (Figure 7A-7C). EEs in these cells remained severely clustered, and none of the Numb isoforms or Numblike could rescue the Mon1b-depletion-induced EE docking defects (Figure 7D and 7E). Moreover, expression of either Numb-65-Δ240-311 or Numb-71-Δ240-311, which are unable to bind Mon1b, could not increase EE fusion (Figure 7F and 7G) or rescue Numb KD-caused EE fusion defects (Figure 7H and 7I). These data together indicate that Numb acts upstream of Mon1b, and Numb-Mon1b association is essential for Numb-mediated EE docking.

Numb- and Mon1b-mediated EE docking is essential for endocytic cargo sorting

EEs are the key endocytic cargo sorting station and have been proposed to be the center of the entire endocytic system [44, 48]. Our data have shown that Numb and Mon1b are docking regulators for EE fusion and both Numb and Mon1b KD resulted in severe EE docking defects. We therefore hypothesized that Numb and Mon1b KD would disrupt endocytic sorting. To test this, we tracked the trafficking route of fluorescently labeled LDL in control, Numb KD and Mon1b KD cells. LDL has been well-documented to be degraded through lysosomes after being internalized into the cell and packed into endocytic vesicles via the classic endocytic pathway [49]. We found that the fluorescence intensity of LDL in control cells gradually decreased during a 180-min chase period after cells were released from the LDL-containing media (~24% retention; Figure 8A and 8B). In contrast, the fluorescence intensity of LDL in Numb or Mon1b KD cells was much more stable within the same chase period (~80% retention; Figure 8A and 8B). This suggests that both Numb and Mon1b KD block LDL trafficking to the lysosome for its degradation. We then performed EEA1 or Lamp1 immunostaining to characterize the retented vesicles. Most of the trapped LDL was enclosed in EEA1-labeled EEs in Numb or Mon1b KD cells after a 15-min chase period, by the time almost half of the LDL had left the EEs in control cells (Figure 8C and 8D). Consistent with this observation, after a 30-min chase period, almost all the LDL in the control cells entered lysosomes for degradation, whereas only half of the LDL in Numb or Mon1b KD cells trafficked to lysosomes (Figure 8E and 8F). These data suggest that Numb and Mon1b KD cause an EE docking defect that severely perturbs the trafficking of LDL towards lysosomes.

To further investigate the impact of Numb and Mon1b KD on endocytic sorting, we used a previously reported assay which tracks the transferrin recycling and LDL degradation simultaneously [50]. It has been shown previously that both internalized transferrin and LDL are transported to EEs via fusion of endocytic vesicles to EEs, and then transferrin is recycled to the plasma membrane while LDL is transported to lysosomes for degradation. Thus, the separation of transferrin and LDL from EEs represents a typical endocytic sorting process. After simultaneous incubation with fluorescent transferrin and LDL, control and Numb KD cells were released and plated in a fresh medium without fluorochrome-tagged ligands and imaged 5 min or 15 min after the release. Both LDL and transferrin were rapidly transported to EEs in the perinuclear region 5 min after the release, and nearly 50% of the LDL-positive vesicles were also transferrin-positive, indicating that a proportion of LDL and transferrin were internalized together into the same endocytic vesicles. Next, we carefully followed the separation of fluorescently labeled transferrin and LDL vesicles, which would reflect the typical sorting process in EEs. At 15 min after the release, almost half of the double-labeled vesicles in control cells separated, as indicated by a ~50% reduction of co-localization of fluorescent transferrin and LDL. However, both Numb and Mon1b depletion markedly blocked/delayed this separation process; only a very slight decrease in the co-localization of fluorescent transferrin and LDL was detected 15 min after the release in Numb KD (~17.5% reduction) and Mon1b KD (~20% reduction) cells. Moreover, we noticed that most co-localized fluorescent transferrin and LDL in either Numb or Mon1b KD cells remained in the perinuclear region, where EEs mostly locate (Figure 8G and 8H), suggesting that the observed sorting blockage is most likely due to EE fusion defects before sorting. These data strongly support that Numb/Mon1b-mediated EE docking and fusion are essential for intracellular signal sorting through

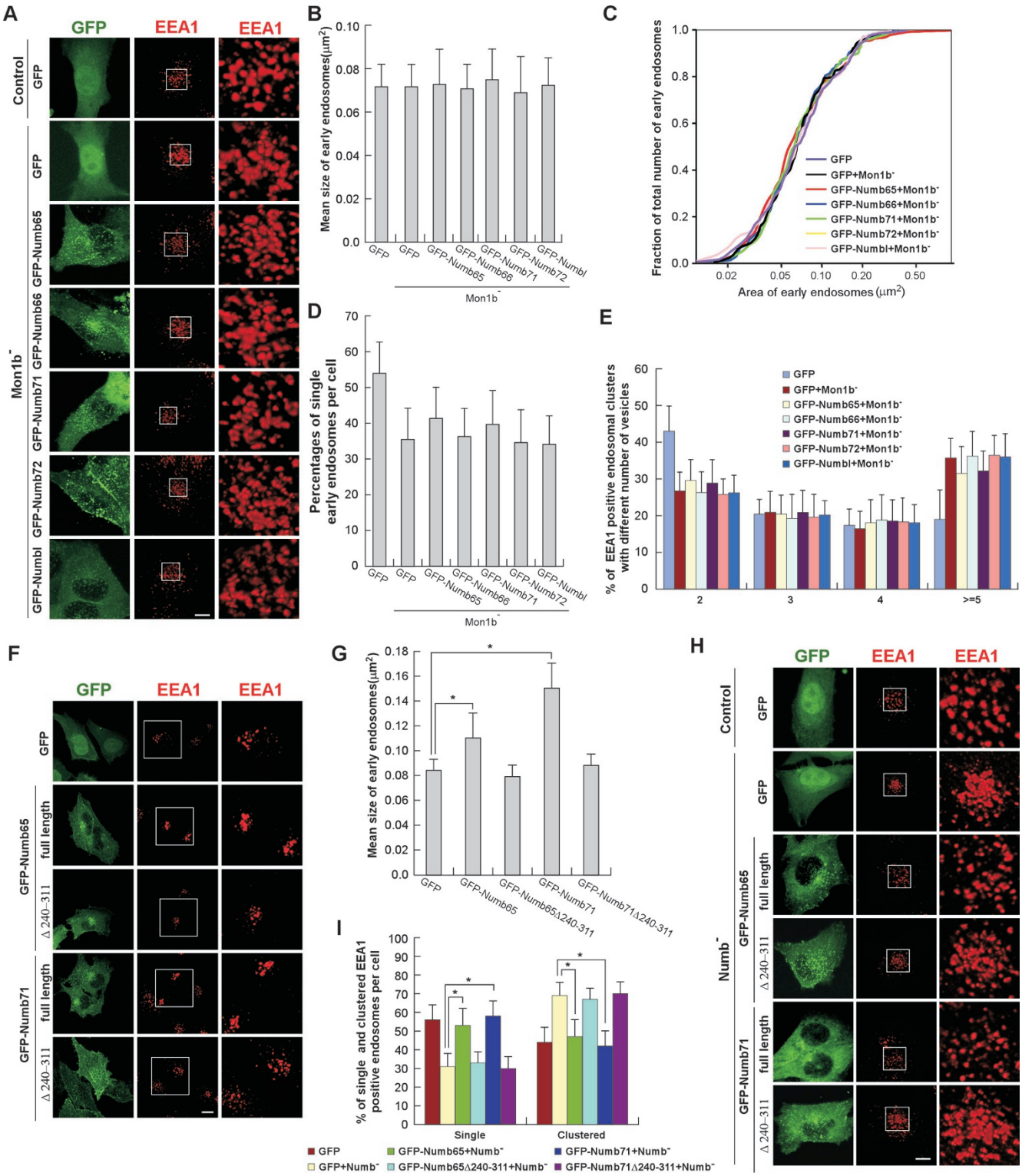

Figure 7 Numb-mediated EE docking is Mon1b-dependent. **(A)** Anti-EEA1 staining of control cells and Mon1b-KD MCF7A cells stably expressing pLKO.1-Mon1b-1 and transiently expressing various Numb and Numblike proteins and quantification of EEA1 vesicles **(B-E)** from 20 cells. **(F, G)** EEA1 immunostaining of MCF7A cells transfected with various constructs indicated in the panel **(F)** and size quantification of EEs (**G**, *n* = 20 cells). **(H, I)** EEA1 immunostaining of control cells and Numb-KD MCF7A cells with various constructs indicated in the panel and quantification of EEs (**I**, *n* = 20 cells). Scale bars, 5 μm.

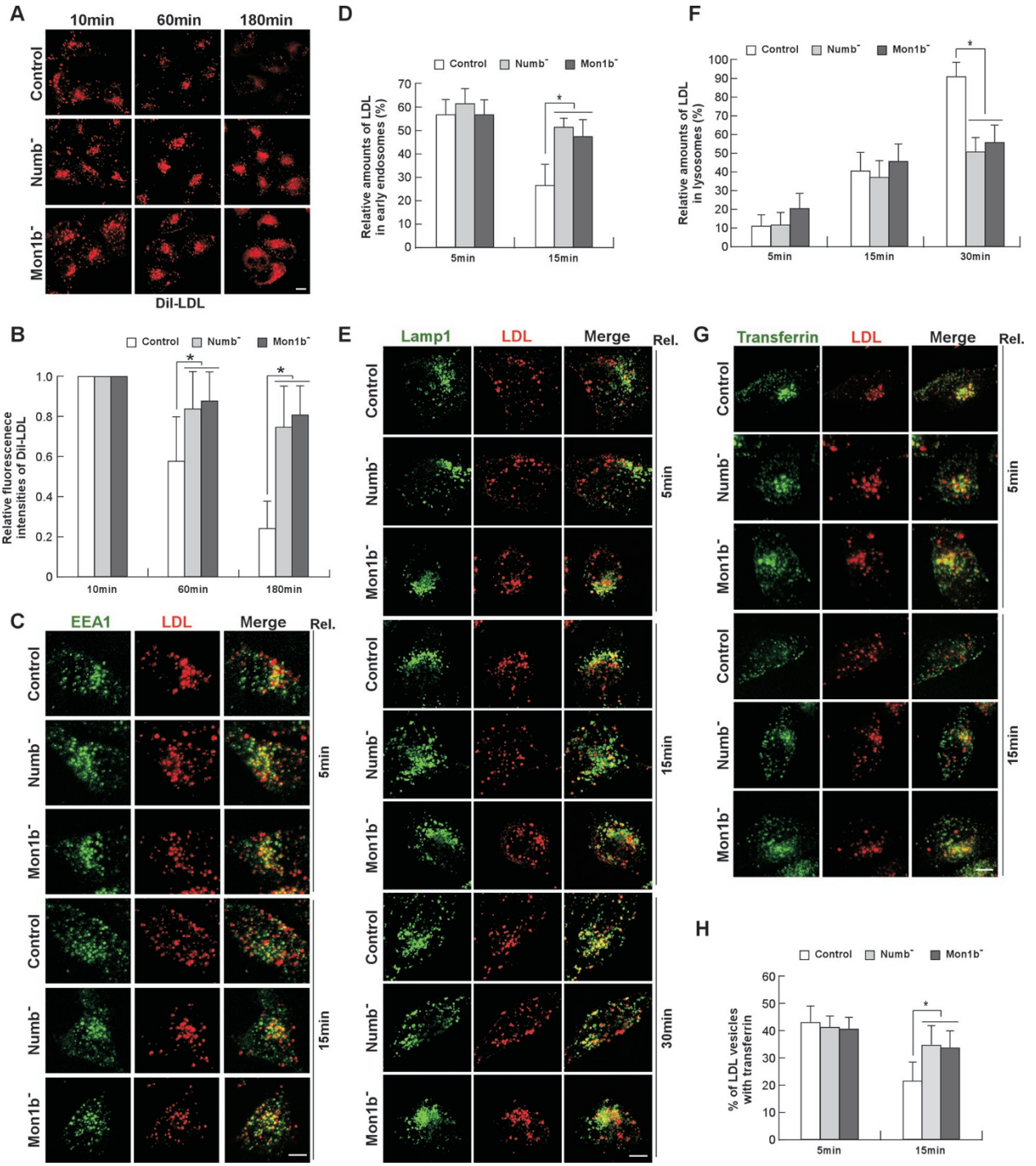

Figure 8 Knockdown of either Numb or Mon1b blocks the endocytic cargo sorting process. **(A**, **B)** Dil-LDL is internalized to control and Numb- or Mon1b-KD MCF7A cells after a 30-min incubation at 37 °C. After 3 washes, cells are released into fresh medium for 10, 60, and 180 min before microscopy **(A)**. Fluorescence intensities of Dil-LDL at each time point are shown in **B**. **(C-F)** Dil-LDL is internalized to control and Numb- or Mon1b-KD MCF7A cells were internalized with Dil-LDL after a 15-min incubation at 4 °C. After 3 washes, cells are incubated in pre-warmed fresh medium for 5 or 15 min at 37 °C and stained with antibodies against EEA1 **(C)** or Lamp1 **(E)**. Percentage of LDL within EEs or lysosomes at each time point is shown in **D** and **F**. **(G**, **H)** Transferrin-488 and Dil-LDL are internalized by control cells and Numb- or Mon1b-KD MCF7A cells for 15 min at 4 °C. After washing, cells are released into pre-warmed fresh media for 5 or 15 min at 37 °C before microscopy **(G)**. Percentage of vesicles positive for both Transferrin-488 and Dil-LDL at each time point is shown in **H**. Scale bars in **A**, 10 μm; scale bars in **C**, **E** and **G**, 5 μm. **P* < 0.01.

the endocytic pathway.

Discussion

Numb plays very important roles as a signaling adaptor in a variety of cellular processes, including cell fate determination, asymmetric cell division, adherens junction maintenance, polarity generation, and cell migration [1-4, 9, 18]. Numb carries out these functions via regulating endocytic trafficking of several key molecules, such as Notch, sanpodo, cadherins and integrins [4, 7, 9, 14, 17, 18, 23, 24, 26, 51, 52]. Although in all these contexts Numb functions as an endocytic adaptor protein, the exact role of Numb in endocytic trafficking remains an open question. Several studies have demonstrated that Numb interacts with two endocytic partners, α-adaptin and Eps15 [26, 27], and is thereby involved in the regulation of clathrin-dependent endocytosis; but whether and how Numb regulates signal molecule degradation and intracellular trafficking through sorting endosomes are not clear. In this study, we unexpectedly identified cytosolic Numb as a novel regulator of EE homotypic fusion. Numb KD severely delays/blocks EE docking. Remarkably, overexpression of only Numb 65 and Numb 71 promotes EE fusion and rescues Numb KD-induced EE fusion defects. Furthermore, cytosolic Numb recruits Mon1b, a homolog of yeast vacuolar tethering/docking protein Mon1, to the EE membrane to promote EE fusion. This finding uncovers a subcellular mechanism by which cytosolic Numb regulates the intracellular signal sorting process. It is plausible that Numb functions as a selective docking factor to allow selected vesicles to fuse with EEs. The signal molecules within these EEs are further transported into late endosomes for degradation or recycled to the plasma membrane via into recycling endosomes, depending on the nature of the signal and the signal strength. In this manner, Numb may selectively regulate various signaling molecules, thereby fulfilling its diverse functions in multiple cellular processes.

All Numb isoforms and Numblike have a C-terminal binding domain for α-adaptin and EPS15 [26, 28], which are responsible for endocytosis, exocytosis and presumably other unidentified types of vesicular trafficking. However, these five Numb proteins have complex structures in their N-terminal domain, which result in distinct subcellular localizations of Numb proteins. Numb 66 and Numb 72 are attached on the plasma membrane and have an 11-aa insertion in the PTB domain. In contrast, Numb 65, Numb 71 and Numblike lack the 11-aa insertion in their PTB domain, and are mostly localized in the cytosol [15, 17]. These observations suggest that the presence of the 11-aa fragment within the PTB domain affects cell membrane localization of Numb proteins. Here, we show that the 11-aa insertion in the PTB domain also determines the role of Numb in the control of endocytic trafficking. We show although all isoforms of Numb and Numblike can bind to Mon1a and Mon1b [36, 47], only Numb 65, Numb 71 and partially Numblike are responsible for EE docking during homotypic fusion. In line with this finding, we observed that Numb 65, Numb 71 and partially Numblike localize on EEs in the perinuclear region, where endocytic sorting occurs in the mammalian cells. These data reveal a novel functional diversity of mammalian Numb proteins during homotypic fusion and cargo sorting process. Our study thus may provide a mechanistic explanation for the different fate of APP in cells expressing Numb with different PTB domains [12].

Interestingly, we found that a truncated PTB domain with deletion of the N-terminal 68-aa region shows stronger localization to EEs (Supplementary information, Figure S6F and S6G). These data suggest that the N-terminal and C-terminal parts of the Numb PTB domain may have different functions in regulating the recruitment of Numb to EEs. The C-terminal part most likely contains a critical domain for EE association, whereas the N-terminal part may regulate this association by modulating the conformation of the PTB domain. The deletion of the N-terminal 68-aa region may completely change the conformation of the PTB domain, allowing it to target to the EEs. It is plausible that the 11-aa insertion in the N-terminal part of the PTB domain may cause subtle yet significant structural change in the PTB domain, precluding its association with EEs.

Previous studies have demonstrated that yeast Mon1 is a crucial tethering/docking factor for homotypic vacuolar fusion. In mammals, two homologs of yeast Mon1 protein, Mon1a and Mon1b, have been characterized. Recent studies have shown that both mammalian Mon1 proteins are located on EEs and act as a switch in the early-to-late endosome transition by controlling the localization of Rab5 and Rab7 GEFs [47]. However, whether the function of Mon1 proteins in vacuolar fusion is conserved in mammals is unknown. In our study, we identified Mon1b as a critical regulator of EE docking, supporting that the Mon1-mediated vacuole membrane fusion is mechanistically conserved in mammals. Surprisingly, Mon1a, unlike Mon1b, does not play a role in EE docking. This is, however, consistent with previous finding that Mon1b, but not Mon1a, is a core component of the class C VPS/HOPS complex [36], which is required for EE homotypic docking and fusion.

How exactly does Numb regulate Mon1b in the regulation of EE docking? Yeast Mon1 is a part of cis-SNARE complex. Mon1 mutation impairs the binding of

Syntaxin to VPS18-a in the C-VPS/HOPS complex and causes improper assembly of the cis-SNARE complex, perturbing the subsequent trans-SNARE pairing during homotypic fusion [36, 53]. It is plausible that cytosolic Numb may bind soluble Mon1b in the cytosol, and then move as a complex to the EE membrane where they regulate the trans-SNARE pairing in homotypic fusion. Considering the conserved function of SNARE cycling in almost all intracellular membrane fusion, we propose that Numb may also be involved in other intracellular membrane fusion events, such as vesicle fission and exocytosis.

How might Numb-mediated EE docking be related to its role in asymmetric cell division of stem cells or progenitor cells? Numb was first recognized as a critical cell fate determinant antagonizing the Notch signaling activity in *Drosophila* [2]. In mammals, four Numb isoforms and Numblike have overlapping and redundant functions, making the roles of Numb in the control of cell fate hard to discern. In mammalian cortical development, Numb was shown to play important roles in maintenance of neural progenitors and adherens junctions, and in neuronal differentiation at different developmental stages [4, 5, 9]. Based on the finding that Numb 71 and Numb 72 are mostly expressed in proliferative cells and Numb 65, Numb 66 and Numblike are mostly expressed in differentiated cells [15, 16], the combinatorial and dynamic expression of the Numb isoforms, each engaging a potentially different array of substrates, would contribute to an enormous diversity of cellular physiology in neural stem cell self-renewal, neural differentiation, and neural regeneration. Based on our results and unpublished data, we propose the following model for the function of mammalian Numb in asymmetric cell division. All isoforms of Numb and Numblike are present in asymmetrically dividing progenitor cells. Owing to an unidentified mechanism, Numb 71 and Numb 72 remain in daughter cells that retain the progenitor cell fate, whereas Numb 65, Numb 66 and Numblike are preferentially sorted to the cells fated for differentiation [15]. In this combinatorial manner, Numb 71 and Numb 72 would regulate factors that maintain stem cell fate and Numb 65, Numb 66 and Numblike would regulate factors that promote neuronal differentiation. At the subcellular level, Numb 65 and Numb 71 regulate signal sorting within EEs, whereas Numb 66 and Numb 72 regulate endocytosis at the plasma membrane. For Notch signaling in asymmetrically dividing progenitors, plasma membrane-attached Numb 66 may facilitate the ubiquitination of Notch by Itch for endocytosis, and cytosolic Numb 65 may sense the density or number of vesicles carrying the internalized Notch and recruit soluble Mon1b to promote EE fusion, preparing for Notch degradation in the differentiating daughter cells [19]. In this scenario, Numb 65 and Mon1b work together in the EEs. Similarly, in the proliferating daughter cells, the plasma membrane-attached Numb 72 facilitates the endocytosis of other receptors for recycling to sustain mitogenic signals, or passes them onto Numb 71 and Mon1b, which mediate an endocytic trafficking pathway that leads to their degradation. Thus, asymmetrically sorted Numb 66 and Numb 65 act at the endocytic step and the EE fusion step, respectively, to propagate the differentiation potential in one half of the cells, whereas Numb 72 and Numb 71 function at these two steps to maintain stem cell or progenitor cell properties in another half of the cells. Consequently, asymmetric daughter cell fates are determined.

In summary, our study uncovers a novel function of two cytosolic isoforms of Numb, which act as docking regulators in EE homotypic fusion and subsequent signal sorting. These findings lay a foundation for exploring more detailed mechanisms of Numb function in the asymmetric cell division of stem cells, in cell survival, as well as in tumorigenesis.

Materials and Methods

Vector construction and RNAi

All Numb and Numblike expression vectors were made by cloning of the full-length or fragments of Numb and Numblike into pcDNA3.1-Myc (Invitrogen) or pEGFP-C2 (Clontech) vectors. Human Mon1A and Mon1B expression vectors were generated similarly. The RFP-Rab5 expression construct was purchased from Addgene (plasmid 14437, generously deposited by Dr Ari Helenius). Q79L and S34N mutants of RFP-Rab5 were generated using the QuickChange Site-Directed Mutagenesis Kit (Stratagene). The shRNA lentiviral constructs used to knockdown human Numb (Cat No RHS4696-99359228 and RHS3979-9576173), Numblike (Cat No RHS3979-97052327), and Mon1b (Cat No RHS3979-9627154 and RHS3979-9627156) were purchased from Open Biosystems. To knock down human Mon1a, we used two shRNA constructsp-GIPZ-Mon1a (Cat No RHS4430-101107193) was purchased from Open Biosystems, and pLKO.1-Mon1a was constructed by our group. The targeted sequence is as follows: GTGCCATCCATAAGCTGATGC.

Cell culture and transfection

MCF 7A cells were cultured in RPMI-1640 medium supplemented with 10% (vol/vol) fetal bovine serum, 100 units/ml penicillin, and 100 units/ml streptomycin at 37 °C in 5% CO_2. HEK293T, Cos7 and primary MEF cells were grown in Dulbecco's modified Eagle medium (DMEM) supplemented with 10% FBS, 2 mM L-glutamine, 1 mM sodium pyruvate and 4.5 mg/ml glucose. Plasmid DNA was transfected using Megtran1.0 (Origene) as described by the manufacturers. Transfected cells were harvested 36 h after transfection and analyzed by immunoprecipitation and western blotting. MCF 7A, HEK293T and Cos7 cells stably expressing various shRNAs were obtained by 2-3 week selection

of transfected cells with 2 μg/ml puromycin.

Antibodies

Rabbit polyclonal antibody against Numb (2756S) was purchased from Cell Signaling. Mouse monoclonal antibody against Numb (MAB4338) was purchased from R&D systems. Antibodies against Myc (2276S), Rab7 (9367S) and Rab11 (5589S) were purchased from Cell Signaling. Rabbit polyclonal antibody (2411S) and mouse monoclonal antibody against EEA1 (ab70521) were purchased from Cell Signaling and Abcam, respectively. Mon1B antibodies were purchased from Novus (NBP1-92131) and Proteintech (17638-1-AP). HGS antibody (H00009146-M01), AP2 antibody (11401-1-AP), Rab4 antibody (07-655), Lamp1 (L1418), Flag antibody (ANT146), HA antibody (MMS-101p), GFP (75-131), actin antibody (sc47778) were purchased from Abnova, Proteintech, Merck Millipore, Sigma, PROSPEC, Covance, NeuroMab, Santa Cruz, respectively. The Mon1A antibody was a kind gift from Dr Fudi Wang (Institute of Nutritional Sciences, CAS, China).

Immunoblotting, immunoprecipitation and immunofluorescence staining

Whole cell lysates were incubated with different antibodies indicated in each experiment at 4 °C for 3 h, followed by 1-h incubation with protein A/G-Sepharose beads. Immunoprecipitated complexes were resolved by SDS-PAGE, and coimmunoprecipitated proteins were detected by western blotting using antibodies indicated in the specific experiments. Antibodies against Numb, Myc, GFP, Flag, HA, Mon1a, and Mon1b were used at 1:1 000 dilution, whereas the antibody against actin was used at 1:5 000.

Immunofluorescence staining was performed as follows. Cells were fixed with 3.7% formaldehyde for 10 min at room temperature, washed 3 times with PBS buffer containing 0.1% Triton X-100, and incubated with the indicated primary antibody for 2 h at room temperature. Cells were washed again and incubated for 1 h at room temperature with the appropriate secondary antibody conjugated to either Alexa Fluor 488 or Alexa Fluor 555 (Invitrogen). For HGS, Mon1a and Mon1b staining, cells were first treated with ice-cold acetone for 30 s before fixation in 3.7% formaldehyde and then were washed and stained as described above. Antibodies against Numb, Mon1a, Mon1b, Rab4, Rab7, Rab11, AP2 and Lamp1 were used at 1:100 dilution, and antibodies against EEA1, Rab5, HGS were used at 1:200 dilution. Anti-Myc antibody was used at 1:1 000 dilution.

In vitro vesicle fusion assay

In vitro vesicle fusion assay was performed as described previously [45]. In brief, control and Numb KD MCF7A cells were incubated with Transferrin-488 or Transferrin-555 for 5 min at 37 °C to internalize these fluorochrome-tagged ligands. Both PNS and cytosol fractions from control and Numb KD cells were prepared and combined for *in vitro* reaction by following the described protocol. Images were acquired on a Zeiss 510 confocal microscope equipped with a PlanApo 63× oil-immersion objective.

Image acquisition and analysis

Immunofluorescence images were acquired on a Zeiss 510 confocal microscope equipped with a PlanApo 63× oil-immersion objective. Further image deconvolution and co-localization analysis were performed using AutoQuant X software (Imaris, Bitplane). Vesicle size measurement was conducted using ImageJ software (Rasband WS, Image J; National Institutes of Health). The cumulative distribution of areas of endosomes/vesicles was analyzed and plotted using R. In each experiment, at least 3 000 vesicles from 10-30 cells were measured. The significance of the difference between a given pair of distributions was determined using the Student's *t*-test. For live-cell imaging, MCF 7A cells seeded on 35-mm culture dishes were either transfected with Rab5-RFP for 24 h or incubated with 50 μg/ml transferrin at 37 °C for 3 min or cultured with 10 μg/ml Di-LDL at 37 °C for 5 min to label early endosomes, as described in the published protocol [45]. After washing with fresh medium for 3 times, cells were immediately imaged on a Nikon ECLIPSE TE200 microscope, equipped with a PlanApo 100× oil-immersion objective. Images were acquired at 5-s intervals for 10 min. Vesicle tracking assignments were performed on all Rab5-, Dil-LDL- and transferrin-labeled endosomes at time = 0 min to monitor their tethering-docking-fusion behaviors during the entire live imaging period.

Electron microscopy

Transmission electron microscopy (EM) was carried out according to standard procedures. Briefly, cells were gently washed with PBS, fixed in 0.1 M phosphate buffer (pH 7.3) containing 2.5% glutaraldehyde for 4 h at 4°C, followed by incubation in 2% aqueous osmium tetroxide for additional 1 h on ice. The cells were then stained with 2% uranyl acetate, dehydrated in a graded ethanol-acetone series, embedded in Spurr's resin, and sliced using an Ultracut-R ultramicrotome (Leica, Germany). EM images were acquired with a Hitachi H-7650 transmission electron microscope. The cumulative distribution of areas of approximately 500 endocytic vesicles from 10 cells was analyzed and plotted by R. The significance of the difference was performed using the Student's *t*-test.

EE isolation

EEs were immunopurified using a slightly modified protocol that was described previously [54]. Briefly, MCF7A or HEK293T cells were homogenized in buffer (250 mM glucose, 3 mM imidazole, and 1 mM EDTA at pH 7.4) containing protease inhibitors by using a glass tissue grinder. Next, PNS was purified by sequential centrifugation of the total cell homogenates for 10 min at 700× g and 30 min at 17 000× g. EEs in PNS were immunoisolated using anti-EEA1 antibodies. Membrane proteins on EEs were detected by immunoblotting as indicated.

FRET measurements

Rab5 activity in living cells was analyzed by a FRET assay, as described previously [43]. Briefly, MCF7A cells seeded on glass dishes were transfected with plasmids CFP-Rab5 and R5BD-YFP. At 24 h after transfection, images of the cells were acquired at room temperature using 2 × 2 binning mode on a Olympus microscope (I×81) equipped with a 100× oil-immersion objective lens, iXon3 EMCCD Camera (Andor Technology) and DV2 Multichannel Imaging System (Photometrics). The filter sets used were YFP (excitation, 500/20 nm; emission, 535/40 nm (DV2)); CFP (excitation, 436/20 nm; emission, 480/30 nm (DV2)); and FRET (excitation, 436/20 nm; emission, 535/40 nm (DV2)). T455Ip (CFP/FRET) and T515Ip (YFP) dichroic mirrors (Chroma) were

used. Corrected FRET ($FRET^C$) and normalized sensitized FRET (FRETN) values were calculated according to the following equations by FRET modules of the xcellence software.

$$FRET^C = FRET - (0.56 \times CFP) - (0.155 \times YFP) \quad (1)$$

$$FRETN = FRET^C / (CFP \times YFP) \quad (2)$$

FRET, CFP and YFP correspond to background-subtracted images of cells co-expressing CFP and YFP acquired through the FRET, CFP and YFP channel, respectively. The values 0.56 and 0.155 are the fractions that were calculated for the bleed-through of CFP and YFP fluorescence, respectively, through the FRET filter channel.

Pseudocolor $FRET^C$ images were obtained by using the xcellence software and were displayed with blue (cold) indicating low values and red (hot) indicating high values.

Endocytosis assays

Endocytosis assays were performed according to the published protocol with minor modification [45, 55]. Briefly, for internalization of fluorochrome-tagged ligands, cells grown on 3.5-cm glass bottom dishes were incubated with 100 μg/ml Alex Fluor 555-transferrin (Invitrogen) or 20 μg/ml Dil-labeled LDL (Invitrogen) for 15 min at 4 °C. After 3 washes with ice-cold PBS, cells were released into 37 °C pre-warmed culture medium, followed by imaging.

Quantitative real-time PCR analysis

Quantitative real time (RT)-PCR reactions were conducted on a CFX96 RT PCR detection system (Bio-Rad). Reaction mixtures were prepared using SsoFast Era Green Supermix (Bio-Rad, Cat No 172-5201AP). Total RNA was prepared using TransZol Up (TransGen Biotech, Cat No ET111-01). First-strand cDNAs were synthesized using TransScript One-step gDNA Removal and cDNA synthesis SuperMix kit (TransGen Biotech, Cat No AT311-02) and served as templates. Nucleotide sequences of the primers used for PCR amplifications were as follows: β-actin，5′-CTCCTCCCTGGAGAAGAGCTA-3′ and 5′-CCTTCTGCATCCTGTCGGCAA-3′; Numb，5′-ACTTTTGATGCTAGTCGGACC-3′ and 5′-GAAGTAGGAGAGGTGGGAGAG-3′; Numblike，5′-TCTCCTTTTGTGCTCCTGAC3-′ and 5′-TTCTCCCGTCGCTGTTTTC-3′; Mon1a，5′-ACACCCTTACCCCTCCAT-3′ and 5′-CTTCTCTTCCTCTGCATGTCAG-3′; and Mon1b，5′-TGGCTGAGAAGGAGACACTAC-3′ and 5′-GGTGGGTAACGAATGAAGAGC-3′.

Acknowledgments

We thank Fudi Wang for Mon1A antibody, Yun Wang and Yuxing Wang for technical support. This work was supported by the Ministry of Science & Technology, China (2014CB964602, 2012CB966802, 2011CB965100, 2010CB945600, 2009CB941402, 2007CB947202, 2013ZX09509104 and 2009R0002), the National Natural Science Foundation of China (31301125, 31071283, 30771102, 81502537, 81370457 and 81271498), China Postdoctoral Science Foundation (2015M572383), Shenzhen Peacock Plan (KQCX20130628112914292), Shenzhen Science and Technology Program (JCYJ20150401145529014 and JCYJ20150630114942300), Shenzhen Key Laboratory for Molecular Biology of Neural Development (ZDSY20120617112838879), SIAT Innovation Program for Excellent Young Researchers (201404 and 201413), and faculty development support (Shenzhen Institutes of Advanced Technology-CAS & Tongji University Shanghai East Hospital).

Author Contributions

HCL and HSL conceived and supervised the study. XMS, YL and QY performed most of the experiments. ZHD, LZ, JCZ and NJ contributed to vector construction and immunoprecipitation experiments. WYQ contributed to electron microscopy experiments. LFG and YJW contributed to statistical analysis of the endosome size. HCL and HSL wrote the manuscript with the assistance from XMS, YL and QY. ZHX, YH, YFM, XQL, CAJ and MYZ provided insightful suggestions and contributed to improving the manuscript.

Competing Financial Interests

The authors declare no competing financial interests.

References

1 Uemura T, Shepherd S, Ackerman L, Jan LY, Jan YN. Numb, a gene required in determination of cell fate during sensory organ formation in *Drosophila* embryos. *Cell* 1989; **58**:349-360.

2 Rhyu MS, Jan LY, Jan YN. Asymmetric distribution of numb protein during division of the sensory organ precursor cell confers distinct fates to daughter cells. *Cell* 1994; **76**:477-491.

3 Knoblich JA, Jan LY, Jan YN. Asymmetric segregation of Numb and Prospero during cell division. *Nature* 1995; **377**:624-627.

4 Li HS, Wang D, Shen Q, *et al.* Inactivation of Numb and Numblike in embryonic dorsal forebrain impairs neurogenesis and disrupts cortical morphogenesis. *Neuron* 2003; **40**:1105-1118.

5 Petersen PH, Zou K, Hwang JK, Jan YN, Zhong W. Progenitor cell maintenance requires numb and numblike during mouse neurogenesis. *Nature* 2002; **419**:929-934.

6 Conboy IM, Rando TA. The regulation of Notch signaling controls satellite cell activation and cell fate determination in postnatal myogenesis. *Dev Cell* 2002; **3**:397-409.

7 Pece S, Serresi M, Santolini E, *et al.* Loss of negative regulation by Numb over Notch is relevant to human breast carcinogenesis. *J Cell Biol* 2004; **167**:215-221.

8 Colaluca IN, Tosoni D, Nuciforo P, *et al.* NUMB controls p53 tumour suppressor activity. *Nature* 2008; **451**:76-80.

9 Rasin MR, Gazula VR, Breunig JJ, *et al.* Numb and Numbl are required for maintenance of cadherin-based adhesion and polarity of neural progenitors. *Nat Neurosci* 2007; **10**:819-827.

10 Cicalese A, Bonizzi G, Pasi CE, *et al.* The tumor suppressor p53 regulates polarity of self-renewing divisions in mammary stem cells. *Cell* 2009; **138**:1083-1095.

11 Kyriazis GA, Wei Z, Vandermey M, *et al.* Numb endocytic adapter proteins regulate the transport and processing of the amyloid precursor protein in an isoform-dependent manner: implications for Alzheimer disease pathogenesis. *J Biol Chem* 2008; **283**:25492-25502.

12 Chan SL, Pedersen WA, Zhu H, Mattson MP. Numb modifies neuronal vulnerability to amyloid beta-peptide in an

isoform-specific manner by a mechanism involving altered calcium homeostasis: implications for neuronal death in Alzheimer's disease. *Neuromolecular Med* 2002; **1**:55-67.
13 Roncarati R, Sestan N, Scheinfeld MH, *et al*. The gamma-secretase-generated intracellular domain of beta-amyloid precursor protein binds Numb and inhibits Notch signaling. *Proc Natl Acad Sci USA* 2002; **99**:7102-7107.
14 Ezratty EJ, Bertaux C, Marcantonio EE, Gundersen GG. Clathrin mediates integrin endocytosis for focal adhesion disassembly in migrating cells. *J Cell Biol* 2009; **187**:733-747.
15 Dho SE, French MB, Woods SA, McGlade CJ. Characterization of four mammalian numb protein isoforms. Identification of cytoplasmic and membrane-associated variants of the phosphotyrosine binding domain. *J Biol Chem* 1999; **274**:33097-33104.
16 Verdi JM, Bashirullah A, Goldhawk DE, *et al.* Distinct human NUMB isoforms regulate differentiation vs. proliferation in the neuronal lineage. *Proc Natl Acad Sci USA* 1999; **96**:10472-10476.
17 Santolini E, Puri C, Salcini AE, *et al.* Numb is an endocytic protein. *J Cell Biol* 2000; **151**:1345-1352.
18 Nishimura T, Kaibuchi K. Numb controls integrin endocytosis for directional cell migration with aPKC and PAR-3. *Dev Cell* 2007; **13**:15-28.
19 McGill MA, McGlade CJ. Mammalian numb proteins promote Notch1 receptor ubiquitination and degradation of the Notch1 intracellular domain. *J Biol Chem* 2003; **278**:23196-23203.
20 Nishimura T, Fukata Y, Kato K, *et al*. CRMP-2 regulates polarized Numb-mediated endocytosis for axon growth. *Nat Cell Biol* 2003; **5**:819-826.
21 Sorensen EB, Conner SD. AAK1 regulates Numb function at an early step in clathrin-mediated endocytosis. *Traffic* 2008; **9**:1791-1800.
22 Spana EP, Doe CQ. Numb antagonizes Notch signaling to specify sibling neuron cell fates. *Neuron* 1996; **17**:21-26.
23 McGill MA, Dho SE, Weinmaster G, McGlade CJ. Numb regulates post-endocytic trafficking and degradation of Notch1. *J Biol Chem* 2009; **284**:26427-26438.
24 Cotton M, Benhra N, Le Borgne R. Numb inhibits the recycling of sanpodo in *Drosophila* sensory organ precursor. *Curr Biol* 2013; **23**:581-587.
25 Scita G, Di Fiore PP. The endocytic matrix. *Nature* 2010; **463**:464-473.
26 Berdnik D, Torok T, Gonzalez-Gaitan M, Knoblich JA. The endocytic protein alpha-Adaptin is required for numb-mediated asymmetric cell division in *Drosophila*. *Dev Cell* 2002; **3**:221-231.
27 Salcini AE, Confalonieri S, Doria M, *et al.* Binding specificity and *in vivo* targets of the EH domain, a novel protein-protein interaction module. *Genes Dev* 1997; **11**:2239-2249.
28 Smith CA, Dho SE, Donaldson J, Tepass U, McGlade CJ. The cell fate determinant numb interacts with EHD/Rme-1 family proteins and has a role in endocytic recycling. *Mol Biol Cell* 2004; **15**:3698-3708.
29 Tokumitsu H, Hatano N, Yokokura S, Sueyoshi Y, Nozaki N, Kobayashi R. Phosphorylation of Numb regulates its interaction with the clathrin-associated adaptor AP-2. *FEBS Lett* 2006; **580**:5797-5801.
30 Bucci C, Parton RG, Mather IH, *et al.* The small GTPase rab5 functions as a regulatory factor in the early endocytic pathway. *Cell* 1992; **70**:715-728.
31 Wickner W. Membrane fusion: five lipids, four SNAREs, three chaperones, two nucleotides, and a Rab, all dancing in a ring on yeast vacuoles. *Annu Rev Cell Dev Biol* 2010; **26**:115-136.
32 McBride HM, Rybin V, Murphy C, Giner A, Teasdale R, Zerial M. Oligomeric complexes link Rab5 effectors with NSF and drive membrane fusion via interactions between EEA1 and syntaxin 13. *Cell* 1999; **98**:377-386.
33 Christoforidis S, McBride HM, Burgoyne RD, Zerial M. The Rab5 effector EEA1 is a core component of endosome docking. *Nature* 1999; **397**:621-625.
34 Rybin V, Ullrich O, Rubino M, *et al.* GTPase activity of Rab5 acts as a timer for endocytic membrane fusion. *Nature* 1996; **383**:266-269.
35 Stenmark H, Vitale G, Ullrich O, Zerial M. Rabaptin-5 is a direct effector of the small GTPase Rab5 in endocytic membrane fusion. *Cell* 1995; **83**:423-432.
36 Wang CW, Stromhaug PE, Kauffman EJ, Weisman LS, Klionsky DJ. Yeast homotypic vacuole fusion requires the Ccz1-Mon1 complex during the tethering/docking stage. *J Cell Biol* 2003; **163**:973-985.
37 Zeigerer A, Gilleron J, Bogorad RL, *et al.* Rab5 is necessary for the biogenesis of the endolysosomal system *in vivo*. *Nature* 2012; **485**:465-470.
38 Elbashir SM, Harborth J, Lendeckel W, Yalcin A, Weber K, Tuschl T. Duplexes of 21-nucleotide RNAs mediate RNA interference in cultured mammalian cells. *Nature* 2001; **411**:494-498.
39 Gauthier NC, Monzo P, Gonzalez T, *et al.* Early endosomes associated with dynamic F-actin structures are required for late trafficking of *H. pylori* VacA toxin. *J Cell Biol* 2007; **177**:343-354.
40 Morel E, Parton RG, Gruenberg J. Annexin A2-dependent polymerization of actin mediates endosome biogenesis. *Dev Cell* 2009; **16**:445-457.
41 Girao H, Geli MI, Idrissi FZ. Actin in the endocytic pathway: from yeast to mammals. *FEBS Lett* 2008; **582**:2112-2119.
42 Hirota Y, Kuronita T, Fujita H, Tanaka Y. A role for Rab5 activity in the biogenesis of endosomal and lysosomal compartments. *Biochem Biophys Res Commun* 2007; **364**:40-47.
43 Galperin E, Sorkin A. Visualization of Rab5 activity in living cells by FRET microscopy and influence of plasma-membrane-targeted Rab5 on clathrin-dependent endocytosis. *J Cell Sci* 2003; **116**:4799-4810.
44 Lakadamyali M, Rust MJ, Zhuang X. Ligands for clathrin-mediated endocytosis are differentially sorted into distinct populations of early endosomes. *Cell* 2006; **124**:997-1009.
45 Barysch SV, Jahn R, Rizzoli SO. A fluorescence-based *in vitro* assay for investigating early endosome dynamics. *Nat Protoc* 2010; **5**:1127-1137.
46 Poteryaev D, Fares H, Bowerman B, Spang A. *Caenorhabditis elegans* SAND-1 is essential for RAB-7 function in endosomal traffic. *EMBO J* 2007; **26**:301-312.
47 Poteryaev D, Datta S, Ackema K, Zerial M, Spang A. Identification of the switch in early-to-late endosome transition. *Cell* 2010; **141**:497-508.

48 Barroso M, Sztul ES. Basolateral to apical transcytosis in polarized cells is indirect and involves BFA and trimeric G protein sensitive passage through the apical endosome. *J Cell Biol* 1994; **124**:83-100.
49 Dunn KW, McGraw TE, Maxfield FR. Iterative fractionation of recycling receptors from lysosomally destined ligands in an early sorting endosome. *J Cell Biol* 1989; **109**:3303-3314.
50 Barysch SV, Aggarwal S, Jahn R, Rizzoli SO. Sorting in early endosomes reveals connections to docking- and fusion-associated factors. *Proc Natl Acad Sci USA* 2009; **106**:9697-9702.
51 Hutterer A, Knoblich JA. Numb and alpha-Adaptin regulate Sanpodo endocytosis to specify cell fate in *Drosophila* external sensory organs. *EMBO Rep* 2005; **6**:836-842.
52 Benhra N, Lallet S, Cotton M, Le Bras S, Dussert A, Le Borgne R. AP-1 controls the trafficking of Notch and Sanpodo toward E-cadherin junctions in sensory organ precursors. *Curr Biol* 2011; **21**:87-95.
53 Sato TK, Rehling P, Peterson MR, Emr SD. Class C Vps protein complex regulates vacuolar SNARE pairing and is required for vesicle docking/fusion. *Mol Cell* 2000; **6**:661-671.
54 de Araujo ME, Huber LA, Stasyk T. Isolation of endocitic organelles by density gradient centrifugation. *Methods Mol Biol* 2008; **424**:317-331.
55 Osborne A, Flett A, Smythe E. Endocytosis assays in intact and permeabilized cells. *Curr Protoc Cell Biol* 2005; Chapter 11:Unit 11.18.

(**Supplementary information** is linked to the online version of the paper on the *Cell Research* website.)